Available online at www.sciencedirect.com
ScienceDirect
International Journal of Mass Spectrometry 261 (2007) 38–44
International Journal of Mass Spectrometry
www.elsevier.com/locate/ijms

# Influence of needle voltage on the formation of negative core ions using atmospheric pressure corona discharge in air☆

Kanako Sekimoto, Mitsuo Takayama*

*International Graduate School of Arts and Sciences, Yokohama City University, 22-2 Seto, Kanazawa-ku, Yokohama, Kanagawa 236-0027, Japan*

Received 20 May 2006; received in revised form 24 July 2006; accepted 24 July 2006
Available online 7 September 2006

**Abstract**

The dependence of the formation of negative core ions $Y^-$ and their hydrated cluster ions $Y^-(H_2O)_n$ on needle voltage has been examined by using atmospheric pressure corona discharge ionization mass spectrometry. An insect pin (200 μm in diameter, 20 mm in length, and ca. 1 μm in the tip radius) was used as the corona needle. At the lowest effective needle voltage (−1.9 kV), water cluster ions $OH^-(H_2O)_n$ with a core ion $OH^-$ were observed. Furthermore there was a discontinuity between the abundances of $OH^-(H_2O)_3$ at *m/z* 71 and $OH^-(H_2O)_4$ at *m/z* 89, suggesting that the cluster $OH^-(H_2O)_3$ is more stable than $OH^-(H_2O)_4$. The ion $OH^-(H_2O)_3$ which may be referred to as "the first hydrated shell" is formed *via* hydration of the core ion $OH^-$ in air. Various different core ions $Y^-$ appeared as the hydrated cluster ions $Y^-(H_2O)_n$ with increasing needle voltage. At relatively low voltage (−2.3 kV), the dominant hydrated clusters observed were $OH^-(H_2O)_n$ and $O_2H^-(H_2O)_n$. At the highest corona voltage (−3.5 kV), the well-known long-lived core ion $NO_3^-$ and its hydrated clusters $NO_3^-(H_2O)_n$ were mainly observed. The resulting negative core ions $OH^-$, $NO_2^-$, $NO_3^-$, $HNO_3^-$, $CO_3^-$, and $CO_4^-$, which are atmospherically important ions or stable terminal ion species in tropospheric atmosphere, are discussed from the standpoint of ion evolution in air.


*Keywords:* Corona discharge; Negative core ion; First hydrated shell; Water cluster

## 1. Introduction

Tropospheric aerosols serve as cloud condensation nuclei, reflect and absorb shortwave solar radiation and thereby influence the earth's climate regulation and radiation budget. A mechanism of aerosol formation in the lower troposphere was proposed by Yu and Turco, and is referred to as "ion-mediated nucleation" [1,2]. The origin of the aerosols is stable core ions that have long lifetimes in air. The core ions are generated by evolution of primary ions through successive ion–molecule reactions with common air constituents and play a central role in aerosol formation. A variety of aerosol formations are dependent on the physical and chemical nature of the individual core ion. In view of their significance, the identification of terminal core ions in air and study of ion evolution have been believed to be important for understanding aerosol formation in the troposphere. There has been significant interest recently in negative air ions due to them having more influence on the earth's environment than positive ions. However, there is relatively little information about negative ion evolution in air.

Fehsenfeld and Ferguson performed kinetic studies on a number of negative ion–molecule reactions with various atmospheric trace gases using a flowing afterglow system [3]. The first in situ mass spectrometric analysis of the negative ions in the troposphere was performed by Heitmann and Arnold [4] and at ground level by Perkins and Eisele [5]. These studies confirmed that there were two hydrated negative ion families with core ions $NO_3^-$ and $HSO_4^-$, i.e., $NO_3^-(HNO_3)_n(H_2O)_m$ and $HSO_4^-(HNO_3)_n(H_2O)_m$ in the troposphere [4] and only $NO_3^-(HNO_3)_n(H_2O)_m$ at the ground level [5]. Kawamoto and Ogawa calculated the fractional abundances of negative ions in the altitude range 0–15 km by simulating elementary processes of negative ion evolution [6]. The computed result showed that cluster ions with the core ions $NO_3^-$, $HSO_4^-$, and $CO_3^-$ were

*Abbreviation:* APCDI, atmospheric pressure corona discharge ionization

☆ This work was presented at the 54th ASMS Conference on Mass Spectrometry, Seattle, Washington, 2006.

* Corresponding author. Tel.: +81 45 787 2431; fax: +81 45 787 2317.
*E-mail address:* takayama@yokohama-cu.ac.jp (M. Takayama).

1387-3806/$ – see front matter © 2006 Elsevier B.V. All rights reserved.
doi:10.1016/j.ijms.2006.07.027

far larger in fractional abundance than other kinds of negative ions. In other work, Luts calculated negative ion evolution up to 100 s by simulating the variations in the concentrations of neutral compounds [7]. He showed that neutral minor constituents such as $HNO_3$ and $H_2SO_4$ participate in the reactions after 0.1 s to form $NO_3^-$ and $HSO_4^-$ ions. According to the directly observed and simultaneous measurement results, the negative core ions $NO_x^-$ and $SO_x^-$, which are well-known air pollutants, have been shown to exist as stable terminal core ions in air.

Mass spectrometric analysis using corona discharge is the most efficient method in the laboratory for the fundamental study of ion evolution in air. A variety of negative core ion species $Y^-$ have been identified by some research groups using corona discharge [8–14] and these are $O^-$, $O_2^-$, $O_3^-$, $CO_3^-$, $CO_4^-$, $NO_2^-$, and $NO_3^-$ and their hydrated clusters $Y^-(H_2O)_n$, while in the case of positive ion, $H_3O^+(H_2O)_n$ is the dominant water cluster ion series under any conditions. The negative ion studies that have been performed have involved different experimental conditions with respect to the discharge pressure [8–11,13], relative humidity [8,10,12], concentration of gases such as ozone and nitrogen oxide [10], discharge current (which depends on the corona needle voltage) [10,11], and ageing time [12]. Skalny et al. remarked in the conclusions of their report [10] that careful control of the gas preparation and input into corona discharge was necessary if reproducible results were to be obtained. The influence of needle voltage on the negative ion formation has been examined by de Vries et al. [14]. They found that the size of water cluster ions decreased with increasing discharge current. Skalny et al. [10] also described that increasing electric field strength led to destruction of cluster ions through collisions with neutral gas due to acceleration of negative cluster ions.

In contrast, the corona current which depends on the needle voltage contributes to the abundances of the discharge by-products such as $O_3$, $NO_x$, and radicals [12,15]. It can be presumed that the corona current or needle voltage affect the formation of the primary ions, as well as the neutral by-products. Further, it is important to note that the electric field strength on a tip of needle depends on the radius, shape, and/or materials of needle tip, because kinetic energy of resulting electrons on the tip may be affecting the formation of primary ions and by-products. When the point tip has the radius of curvature $R$, the field strength can be expressed by $2V/R \log(4d/R)$ [16]. The variables $V$ and $d$ represent the needle voltage and the discharge gap between the tip and orifice plate, respectively. Here we used an insect pin made of stainless steel as the negative corona needle with radius of ca. 1 μm, while Skalny et al. have used a tip made of Pt wire with radius of 100 μm [10]. Although it will be seen that the results of different two experiments are difficult to compare to each other, here we describe the influence of the needle voltage on the formation of negative core ions in ambient air, by using atmospheric pressure corona discharge ionization mass spectrometry (APCDI MS). The use of the insect pin as the needle for negative corona discharge successfully led to regular and reproducible generation of various different negative core ions $Y^-$ and their hydrated cluster ions $Y^-(H_2O)_n$. In the work described here we concentrate on the formation of core ions $OH^-$, $NO_x^-$, and $CO_x^-$.

## 2. Experimental

Mass spectra were acquired on a JMS-LCmate reversed geometry double-focusing mass spectrometer (JEOL, Tokyo, Japan), under ambient air with relative humidity of 25% at 24 °C. The relative humidity was adjusted with an automatic humidity controlled cabinet Dry-Cabi TS-81B-HU (Tolihan Corp., Tokyo, Japan). The ion source was covered with the cabinet. A schematic illustration of the ion source is shown in Fig. 1. The ion source contained a discharge needle made of stainless steel with a diameter of 200 μm and 20 mm in length. The needle used was an insect pin with headless named Bishin (Shiga, Tokyo, Japan). The needle tip with glossy surface as a point electrode was ca. 1 μm in the radius of curvature. The distance between the needle tip and the orifice plate was 3 mm. The orifice (130 μm in i.d. and 5 mm in length) was formed by a stainless tube. Discharge voltages over the range −1.9 to −3.6 kV were applied to the needle relative to the orifice plate. The ions formed

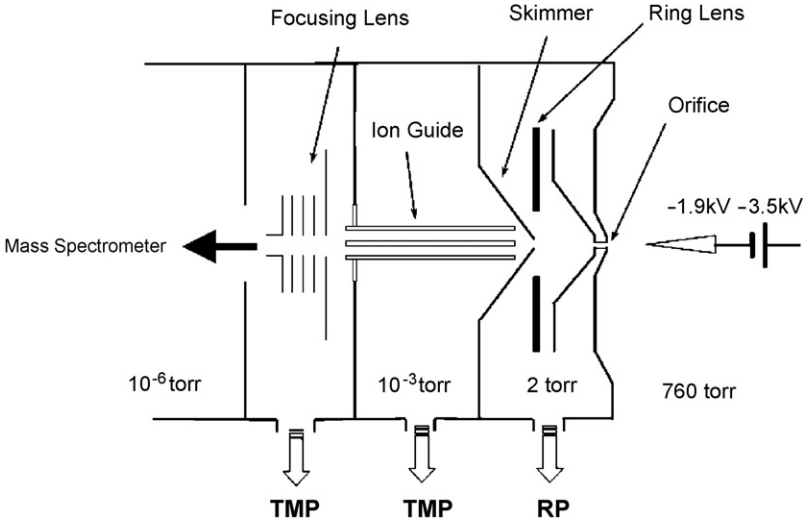


Fig. 1. Schematic illustration of the ion-source in APCDI MS.

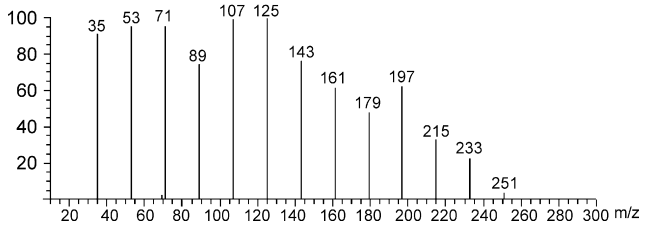


Fig. 2. Negative ion APCDI mass spectrum at a needle voltage of −1.9 kV in ambient air with relative humidity of 25% at 24 °C.

enter the orifice and expand together with air in the intermediate region between orifice and skimmer, which was maintained at 0.27 kPa. The ions were focused onto the skimmer opening (1 mm in diameter) by the ring lens and were transported into the focus lenses region *via* the ion guide. The voltage applied to the skimmer and ring lens were 25 and 50 V, respectively. The applied voltage on the ion guide was 2.56 kV. The transported ions were accelerated to 2.5 kV at the focusing lens electrode and separated by the reversed geometry double-focusing mass spectrometer. The scan speed was 5 s/scan. The reproducibility of mass spectral patterns was confirmed. Gases in the laboratory and ambient air were used without any preparation.

## 3. Results and discussion

### 3.1. Water cluster ions with the core ion $OH^-$

At voltages that produce effective corona discharge (−1.9 kV or above), stable distribution mass spectra consisting of water cluster ions $Y^-(H_2O)_n$ with core ions $Y^-$ were obtained. At voltages below −1.9 kV, ion peaks were not observed. The "core ion $Y^-$" refers to the origin of the water cluster ions $Y^-(H_2O)_n$, that is, the lowest mass peak in the series of water cluster ions corresponds to the core ion, although the peak of core ions $Y^-$ is not always observed. The mass spectrum obtained at the lowest corona voltage (−1.9 kV) in ambient air with relative humidity of 25% at 24 °C showed water cluster ion peaks of $OH^-(H_2O)_n$ ($n$ = 1–13) with a core ion $OH^-$, as shown in Fig. 2. In higher humidity (50%), a core ion peak at $m/z$ 17 was observed as shown in Fig. 3. The dominance of hydrated cluster ions $OH^-(H_2O)_n$ at the lowest voltage was independent of relative humidity conditions. Nagato et al. [12] also observed this ion series with an ion reaction time of $10^{-3}$ s using purified air. They described that the relative abundance of the cluster ions $OH^-(H_2O)_n$ increased with increasing concentration of $H_2O$ vapor.

In the distribution of $OH^-(H_2O)_n$, a reproducible discontinuity from $OH^-(H_2O)_3$ at $m/z$ 71 to $OH^-(H_2O)_4$ at $m/z$ 89 was observed in both mass spectra obtained under different relative humidity. This anomalous distribution is similar to that between the well-known positive ion magic cluster $H_3O^+(H_2O)_{20}$ and $H_3O^+(H_2O)_{21}$ which indicates that $H_3O^+(H_2O)_{20}$ is more stable than $H_3O^+(H_2O)_{21}$ [17]. Thus our results indicate that the $OH^-(H_2O)_3$ ion is more stable than $OH^-(H_2O)_4$ ion. This is direct mass spectrometric evidence for the Eigen postulation that $OH^-(H_2O)_3$ ($m/z$ 71) in negative ion is corresponding to $H_3O^+(H_2O)_3$ ($m/z$ 73) in positive ion which is a particularly stable form consisting of "secondary hydration shell" he called [18]. These stable ions may be called the "first hydrated shell" and are formed by the core ions $OH^-$ and $H_3O^+$ becoming hydrated with water vapor in air. The higher stability of first hydrated shells $H_3O^+(H_2O)_3$ and $OH^-(H_2O)_4$ compared to other size water cluster ions was first confirmed by discontinuity in the van't Hoff plots for the $H_3O^+(H_2O)_n$ [19] and $OH^-(H_2O)_n$ [20], respectively. Robertson et al. [21] reported the vibrational spectroscopic confirmation of the $OH^-(H_2O)_3$ and $OH^-(H_2O)_4$ clusters selected with a tandem time-of-flight mass spectrometer. On the basis of the spectroscopic data, they displayed structures of $OH^-(H_2O)_3$ and $OH^-(H_2O)_4$ clusters having a $C_3$ symmetry or pyramidal conformation, by using *ab initio* calculation. In the latest report, Pickard et al. [22] have demonstrated good comparison of the four *ab initio* calculations for hydrated shells $H_3O^+(H_2O)_n$ ($n$ = 1–3) and $OH^-(H_2O)_n$ ($n$ = 1–4) with experimental data of $\Delta H^\circ$ and $\Delta G^\circ$. The GAUSSIAN 2 and GAUSSIAN 3 calculations for $OH^-(H_2O)_n$ ($n$ = 1–4) clusters have successfully predicted the discontinuity from $OH^-(H_2O)_3$ to $OH^-(H_2O)_4$.

The formation mechanism of $OH^-(H_2O)_n$ can be explained on the basis of the kinetic study by Fehsenfeld and Ferguson [3]. According to their study, the ion–molecule reactions which form $OH^-(H_2O)_n$ can be described as below. Generally, corona discharge produces $O_2^{\bullet+}$ and $N_2^{\bullet+}$ in ambient air, i.e.,

$$N_2 + e^- \rightarrow N_2^{\bullet+} + 2e^- \quad (1\text{-}1)$$

$$O_2 + e^- \rightarrow O_2^{\bullet+} + 2e^- \quad (1\text{-}2)$$

The resulting electrons have a distribution of kinetic energy. In the case of low energetic electrons, electron attachment occurs on $O_2$ (reaction b in Fig. 6) and the attachment of high energetic electrons brings about a dissociative attachment reaction (reaction a in Fig. 6) as expressed by the reactions (2) and (3),

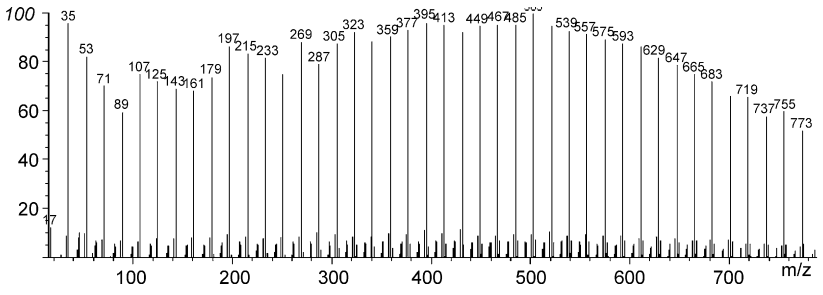


Fig. 3. Negative ion APCDI mass spectrum at a needle voltage of −1.9 kV in ambient air with relative humidity of 50% at 24 °C.

respectively.

$$O_2 + e^- \rightarrow O_2^- \quad (2)$$

$$O_2 + e^- \rightarrow O_2^{-*} \rightarrow O^- + O \quad (3)$$

If abundant $H_2O$ molecules are present in air, another dissociative attachment reaction may occur on $H_2O$ to produce $OH^-$ [8] (reaction e in Fig. 6).

$$H_2O + e^- \rightarrow OH^- + H \quad (4)$$

The products $O_2^-$ and $O^-$ are known as the primary ions for the negative ion evolution in air. The ion $O^-$ is the primary ion for the formation of $OH^-(H_2O)_n$. The following three-body reactions (5) and (6) and binary reaction (7) of $O^-$ produce $O^-(H_2O)$, $CO_3^-$, and $OH^-$ competitively.

$$O^- + H_2O + O_2 \rightarrow O^-(H_2O) + O_2 \quad (5)$$

$$O^- + CO_2 + O_2 \rightarrow CO_3^- + O_2 \quad (6)$$

$$O^- + H_2O \rightarrow OH^- + OH \quad (7)$$

The rate constants of reactions (5)–(7) are $k_{(5)} = 1.3 \times 10^{-28}$ cm$^6$/s, $k_{(6)} = 3.1 \times 10^{-28}$ cm$^6$/s, and $k_{(7)} < 6 \times 10^{-13}$ cm$^6$/s, respectively [3]. Taking into account the air constituents, the three-body reactions with $O_2$ as the third body do occur, though the probability of three-body reactions is negligibly small compared to binary reactions. The product ion of reaction (5), $O^-(H_2O)$, is better described as $OH^-(OH)$ which is a lower energy form. Since atmospheric ambient air contains abundant $O_2$ and trace amount of $CO_2$, $O^-(H_2O)$ is likely to be produced more than the product ions of reaction (6) $CO_3^-$. The ion $O^-(H_2O)$ was efficiently converted *via* the fast binary reaction (8) to form a hydrate $OH^-(H_2O)$. Following hydration, reactions of $OH^-$ and $OH^-(H_2O)$, produced by reactions (4), (7), and (8), to form the "first hydrated shell" may occur in air.

$$O^-(H_2O) + H_2O \rightarrow OH^-(H_2O) + OH \quad (8)$$

$$OH^- + n(H_2O) \rightarrow OH^-(H_2O)_n \quad (n \leq 3) \quad (9)$$

$$OH^-(H_2O) + n(H_2O) \rightarrow OH^-(H_2O)_{n+1} \quad (n \leq 2) \quad (9')$$

After the ion species resulting from the ion evolution were introduced into the vacuum region, the further clustering reaction with $H_2O$ may occur successively by adiabatic expansion as follows.

$$OH^-(H_2O)_{n+1} + m(H_2O) \rightarrow OH^-(H_2O)_{n+m+1} \quad (10)$$

### 3.2. The influence of needle voltage on the formation of negative core ions

Negative water cluster ions $Y^-(H_2O)_n$ varied considerably in pattern with increasing needle voltage. The various different core ions or their hydrates appeared successively and the abundances of those ions changed with an increase in voltage from −1.9 to −3.5 kV, while the positive cluster ions $H_3O^+(H_2O)_n$ were invariant with change in voltage. At a voltage of −3.6 kV, the corona discharge discontinuously transferred to the discharge

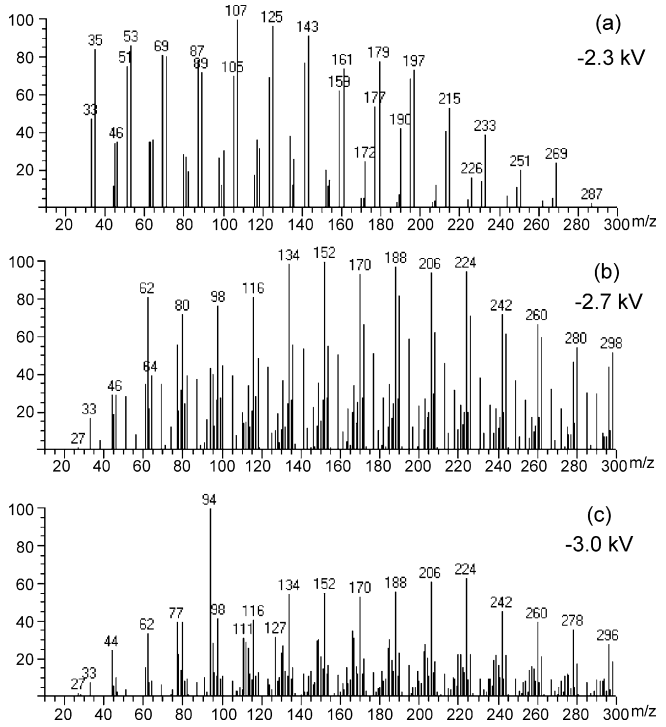


Fig. 4. Negative ion APCDI mass spectra at needle voltages of (a) −2.3, (b) −2.7, and (c) −3.0 kV in ambient air with relative humidity of 25% at 24 °C.

by an arc. Negative ion APCDI mass spectra obtained at needle voltages of −2.3, −2.7, and −3.0 kV are shown in Fig. 4(a–c), respectively. The ion peaks at *m/z* 33, 44, and 46 appeared in the mass spectrum at −2.3 kV and can be assigned as the core ions or hydrate $O_2H^-$, $N_2O^-$ or $CN^-(H_2O)$, and $NO_2^-$, respectively. The formation of a core ion $CO_2^-$ (*m/z* 44) has not been observed thus far. The mass spectrum shows the ions of the dominant series $OH^-(H_2O)_n$ and $O_2H^-(H_2O)_n$ and the minor cluster $N_2O^-(H_2O)_n$ or $CN^-(H_2O)_n$. At a medium voltage of −2.7 kV, an abundant ion at *m/z* 62 and a minor peak at *m/z* 27 ($HCN^-$) appeared in the low-mass region. The ion at *m/z* 62 could correspond to hydrates $CN^-(H_2O)_2$ or $N_2O^-(H_2O)$, or a core ion $NO_3^-$. Considering that $NO_3^-$ is a well-known stable terminal ion in air [12,13], it is likely that the dominant core ion and its hydrated cluster observed in the mass spectrum at −2.7 kV is the $NO_3^-$ and $NO_3^-(H_2O)_n$, respectively. The outstanding peak at *m/z* 94 observed in Fig. 4(c) could not be assigned.

In order to estimate the change in the appearance and abundance of typical core ions with varying needle voltages, the peaks at *m/z* 35, 46, 62, 63, 78, and 112, which correspond to the well-known core ions or hydrated ions $OH^-(H_2O)$, $NO_2^-$, $NO_3^-$, $HNO_3^-$, $CO_3^-(H_2O)$, and $CO_4^-(H_2O)_2$ respectively, were concentrated on. These core ions have been reported in previous studies using corona discharge [8–13]. Fig. 5 shows the influence of needle voltage on the absolute abundances of those negative core or hydrated ions. Negative core or hydrated ions used here to make Fig. 5 are listed in Table 1 together with corresponding *m/z* values. The water cluster ions $OH^-(H_2O)_n$ were dominant from the lowest voltage of −1.9 up to −2.3 kV. The abundance of the cluster ions $OH^-(H_2O)_n$ started to decrease at −2.3 kV and had disappeared by −2.6 kV. Instead, the cluster

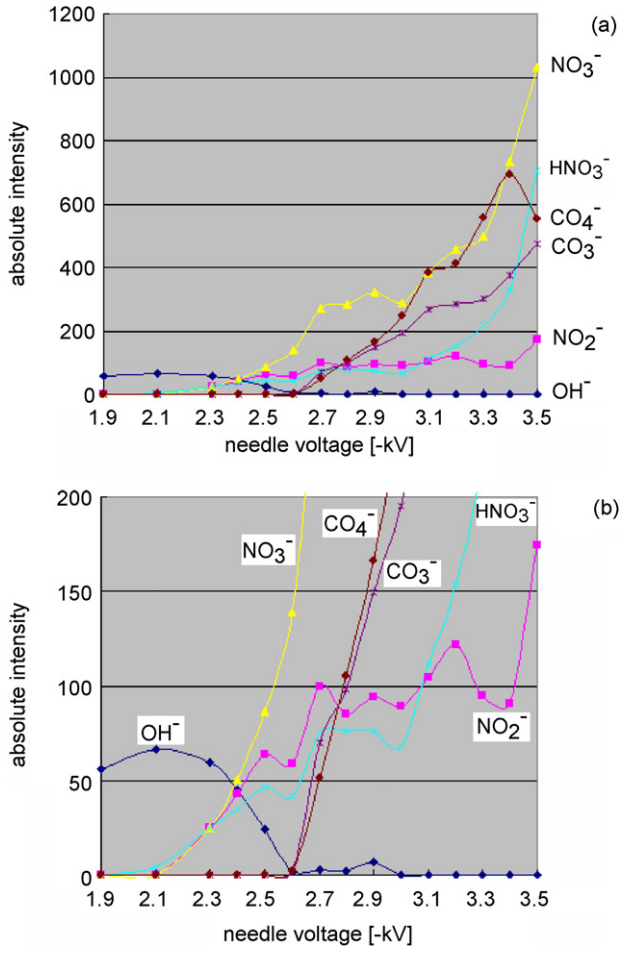


Fig. 5. (a) Influence of the needle voltage on the absolute abundance of the different negative core ions $OH^-$, $NO_2^-$, $NO_3^-$, $HNO_3^-$, $CO_3^-$, and $CO_4^-$ and (b) an enlargement in the vertical axis.

ions $CO_3^-(H_2O)_n$ and $CO_4^-(H_2O)_n$ with other core ions $CO_3^-$ and $CO_4^-$ appeared at −2.6 kV and increased continuously up to the highest corona voltage (−3.5 kV). Furthermore, the alternative series cluster ions $NO_2^-(H_2O)_n$, and $NO_3^-(H_2O)_n$ appeared at −2.1 kV with the absolute abundances increasing over the range −2.1 to −2.7 kV, with a remarkable increase at −2.6 kV. The abundances of $NO_2^-(H_2O)_n$ and $NO_3^-(H_2O)_n$ were constant from −2.7 to −3.5 kV and −3.0 kV, respectively. The ions $HNO_3^-$ and $NO_3^-(H_2O)_n$ started to increase in abundance considerably at −3.0 kV. At voltages above −2.5 kV, $NO_3^-(H_2O)_n$ was the dominant series. With the exception of the cluster ions $OH^-(H_2O)_n$, the ion abundance of all the ion species increased dramatically at −2.6 kV.

Table 1
Observed negative core or hydrated ions used to make Fig. 5 and corresponding *m*/*z* values

| Core or hydrated ions | *m*/*z* value |
|---|---|
| $OH^-$ | 17 |
| $HCN^-$ | 27 |
| $O_2H^-$ | 33 |
| $N_2O^-$ | 44 |
| $NO_2^-$ | 46 |
| $NO_3^-$ | 62 |
| $HNO_3^-$ | 63 |
| $CO_3^-(H_2O)$ | 78 |
| $CO_4^-(H_2O)_2$ | 112 |

Table 2
Elementary processes for the formation of negative core ions $OH^-$, $NO_2^-$, $NO_3^-$, $HNO_3^-$, $CO_3^-$, and $CO_4^-$ in air and the rate constant for each process

| | |
|---|---|
| a: $O_2 + e^- \rightarrow O_2^{-*} \rightarrow O^- + O$ | |
| a-1: $O^- + H_2O + O_2 \rightarrow O^-(H_2O) + O_2$ | $1.3 \times 10^{-28}$ cm$^6$/s |
| $O^-(H_2O) + H_2O \rightarrow OH^-(H_2O) + OH$ | $>1 \times 10^{-11}$ cm$^3$/s |
| $OH^-(H_2O)_n + H_2O \rightarrow OH^-(H_2O)_{n+1}$ | Clustering reaction |
| a-2: $O^- + CO_2 + O_2 \rightarrow O^-(CO_2) + O_2$ | $3.1 \times 10^{-28}$ cm$^6$/s |
| $CO_3^-(H_2O)_n + H_2O \rightarrow CO_3^-(H_2O)_{n+1}$ | Clustering reaction |
| a-1-2: | $<1.5 \times 10^{-11}$ cm$^3$/s |
| $OH^-(H_2O)_n + NO_2 \rightarrow NO_2^-(H_2O)_{n-1} + OH + H_2O$ | |
| a-2-1: $CO_3^-(H_2O)_n + NO \rightarrow NO_2^-(H_2O)_n + CO_2$ | |
| $CO_3^-(H_2O) + NO \rightarrow NO_2^-(H_2O) + CO_2$ | $\sim 7 \times 10^{-12}$ cm$^3$/s |
| $NO_2^-(H_2O)_n + H_2O \rightarrow NO_2^-(H_2O)_{n+1}$ | Clustering reaction |
| a-2-2: $CO_3^-(H_2O)_n + NO_2 \rightarrow NO_3^-(H_2O)_n + CO_2$ | |
| $CO_3^- + NO_2 \rightarrow NO_3^- + CO_2$ | $2 \times 10^{-10}$ cm$^3$/s |
| $NO_3^-(H_2O)_n + H_2O \rightarrow NO_3^-(H_2O)_{n+1}$ | Clustering reaction |
| b: $O_2 + e^- \rightarrow O_2^-$ | |
| b-1: $O_2^-(H_2O)_n + H_2O \rightarrow O_2^-(H_2O)_{n+1}$ | Clustering reaction |
| b-2: $O_2^- + CO_2 + O_2 \rightarrow O_2^-(CO_2) + O_2$ | $4.7 \times 10^{-29}$ cm$^6$/s |
| $CO_4^-(H_2O)_n + H_2O \rightarrow CO_4^-(H_2O)_{n+1}$ | Clustering reaction |
| b-1-1: $O_2^-(H_2O)_n + NO \rightarrow NO_3^-(H_2O)_n$ | |
| $O_2^-(H_2O) + NO \rightarrow O_2^-(NO) + H_2O$ | $3.1 \times 10^{-10}$ cm$^3$/s |
| $NO_3^-(H_2O)_n + H_2O \rightarrow NO_3^-(H_2O)_{n+1}$ | Clustering reaction |
| b-1-2: $O_2^-(H_2O)_n + NO_2 \rightarrow NO_2^-(H_2O)_n + O_2$ | |
| $O_2^- + NO_2 \rightarrow NO_2^- + O_2$ | $1.2 \times 10^{-9}$ cm$^3$/s |
| $NO_2^-(H_2O)_n + H_2O \rightarrow NO_2^-(H_2O)_{n+1}$ | Clustering reaction |
| b-2-1: $CO_4^-(H_2O)_n + NO \rightarrow NO_3^-(H_2O)_n + CO_2$ | |
| $CO_4^- + NO \rightarrow O^-(ONO) + CO_2$ | $4.8 \times 10^{-10}$ cm$^3$/s |
| $NO_3^-(H_2O)_n + H_2O \rightarrow NO_3^-(H_2O)_{n+1}$ | Clustering reaction |
| c: $NO_2^-(H_2O)_n + NO_2 \rightarrow NO_3^-(H_2O)_n + NO$ | $4 \times 10^{-12}$ cm$^3$/s |
| $NO_2^- + NO_2 \rightarrow NO_3^- + NO$ | |
| $NO_3^-(H_2O)_n + H_2O \rightarrow NO_3^-(H_2O)_{n+1}$ | Clustering reaction |
| d-1: $NO_2 + OH + M \rightarrow HNO_3 + M$ (M: a third body) | |
| d-2: $HNO_3 + e^- \rightarrow HNO_3^-$ | |
| d-3: $HNO_3 + NO_2^-(H_2O)_n \rightarrow NO_3^-(H_2O)_n + HNO_2$ | |
| $NO_2^- + HNO_3 \rightarrow NO_3^- + HNO_2$ | $1.6 \times 10^{-9}$ cm$^3$/s |
| $NO_3^-(H_2O)_n + H_2O \rightarrow NO_3^-(H_2O)_{n+1}$ | Clustering reaction |
| e: $H_2O + e^- \rightarrow OH^- + H$ | |
| $OH^-(H_2O)_n + H_2O \rightarrow OH^-(H_2O)_{n+1}$ | Clustering reaction |

According to the results obtained here and in previous studies [3,8,10,12,23,25], the sequence of ion–molecule reactions involving all cluster ions $Y^-(H_2O)_n$ described above can be illustrated as shown in Fig. 6. Elementary processes and corresponding rate constants for the ion evolution listed in Table 2 can be estimated from the results presented here and in previous studies [3,8,10,12,23–25]. It is postulated that growth of the water clusters with different core ions in the hydration reactions a-1, b-1, and b-2 may occurs *via* adiabatic expansion. It is likely that sequential progress of the reactions would be regulated by needle voltage. At the lowest voltage (−1.9 kV), it was presumed that $CO_3^-(H_2O)_n$, $CO_4^-(H_2O)_n$, and $O_2^-(H_2O)_n$ formed in

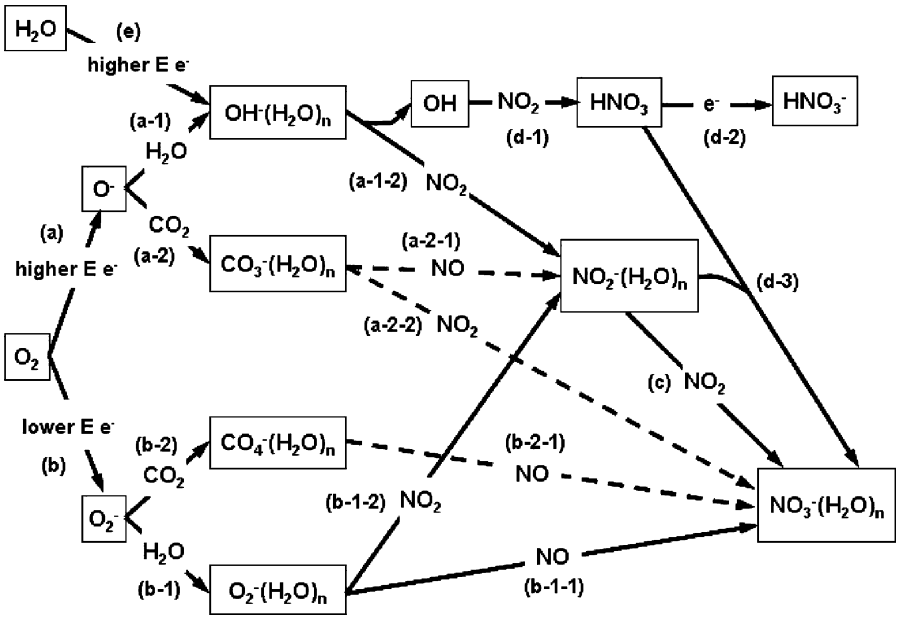


Fig. 6. Proposed sequential progress of the ion–molecule reactions for the water clusters $Y^-(H_2O)_n$ with different negative core ions $OH^-$, $NO_2^-$, $CO_3^-$, $NO_3^-$, $HNO_3^-$, and $CO_4^-$.

addition to $OH^-(H_2O)_n$, although those ion series were not observed here. In Fig. 6, reactions a-2 and b-2 which produce $CO_3^-(H_2O)_n$ and $CO_4^-(H_2O)_n$ are likely to be less dominant than reactions a-1 and b-1 which produce $OH^-(H_2O)_n$ and $O_2^-(H_2O)_n$ at the low voltage, because ambient air has a lower abundance of $CO_2$ than of $H_2O$. The cluster ion $O_2^-(H_2O)_n$ was not observed at any voltage. Nagato et al. [12] described that $O_2^-(H_2O)_n$ were the terminal ions formed in a time shorter than $10^{-5}$ s and that $OH^-(H_2O)_n$ was observed at a reaction time of $10^{-3}$ s. Skalny et al. [10] observed trace amounts of the ion series $O_2^-(H_2O)_n$ at a pressure of 27 kPa in wet air with a relative humidity 40–55%. The ion transport time between the electrodes in their experiments was of the order of $10^{-5}$ s. The above reports by Nagato et al. [12] and Skalny et al. [10] indicate that the life time of the $O_2^-(H_2O)_n$ ion is shorter than that of the $OH^-(H_2O)_n$ ion. It is suggested from these reports that the experimental conditions described here are suitable for detecting the core ions formed in a reaction time greater than $10^{-3}$ s.

The neutral species $NO_x$ are involved in all reactions to form $NO_2^-(H_2O)_n$ and $NO_3^-(H_2O)_n$. Sufficient abundance of $NO_x$ in air is absolutely necessary to observe these cluster ion series in mass spectra. $NO_x$ are produced as one of the by-products of discharge. The neutral NO is formed from nitrogen and oxygen atoms produced by electron impact dissociation in the corona discharge [10]. The NO formation can be attributed to the electron kinetic energy which depends on electric field strength on the tip of the needle. The neutral $NO_2$ is produced by oxidation of NO. The appearance of the cluster ions $NO_2^-(H_2O)_n$ and $NO_3^-(H_2O)_n$ at −2.1 kV suggests that the kinetic energy of electrons at a needle voltage of −2.1 kV reaches the threshold sufficient to generate $NO_x$. Electron affinities of $NO_2$ (2.04 eV) and $NO_3$ (3.93 eV) are generally greater than those of other neutral species in air. These ions are apt to become stable negative ions *via* charge transfer reactions with other negative ions. The cluster ions $NO_3^-(H_2O)_n$ have been regarded as the most stable negative ions among atmospheric species. Nagato et al. [12] reported that the production of $NO_3^-$ proceeded with increasing ion reaction time in air. It is evident that $NO_3^-$ is the longest-lived negative ion species in air.

The absolute abundances of $NO_2^-(H_2O)_n$ and $NO_3^-(H_2O)_n$ increased as that of $OH^-(H_2O)_n$ simultaneously decreased, as shown in Fig. 5(b). This fact suggests that the charge transfer reaction a-1-2 of $OH^-$ with $NO_2$ may easily occur, because the electron affinity of OH (1.83 kV) is lower than that of $NO_2$. Another charge transfer reaction, namely b-1-2 of $O_2^-$ with $NO_2$ may take place due to lower electron affinity of $O_2$ (0.48 eV) compared to that of $NO_2$, although both $O_2^-$ and its hydrate $O_2^-(H_2O)_n$ were not observed here. The ions $NO_2^-(H_2O)_n$ and $NO_3^-(H_2O)_n$ have also been observed in other experiments using corona discharge [8,10,12,13]. Skalny et al. [10] observed the $NO_3^-(H_2O)_n$ growth with time at a pressure of 27 kPa under static conditions, in which air flow was stopped. A concomitant increase with time in the concentrations of by-products produced in the static discharge was observed. The ion series was not observed in an air flowing regime. Shahin [8] reported that $NO_2^-(H_2O)_n$ and $NO_3^-(H_2O)_n$ were detected predominantly at lower pressure in the discharge tube. This observation was explained by the fact that relative concentration of $NO_2$ produced by discharge increased with decreasing the pressure.

The abundances of the cluster ions $NO_2^-(H_2O)_n$, $NO_3^-(H_2O)_n$, $CO_3^-(H_2O)_n$, and $CO_4^-(H_2O)_n$ increased drastically at −2.6 kV (Fig. 5(b)). This observation suggests that all the reactions mentioned above were promoted due to the great enhancement of the production of primary ions at −2.6 kV. The reason why the abundance of $OH^-(H_2O)_n$ alone does not increase at −2.6 kV is that $OH^-(H_2O)_n$ is converted completely to $NO_2^-(H_2O)_n$ *via* charge transfer reaction a-1-2. It was

expected that the abundance of all ion species would increase continuously at voltages above −2.6 kV. However, the increase of $NO_2^-(H_2O)_n$ and $NO_3^-(H_2O)_n$ stopped at −2.7 kV, while the abundance of $CO_3^-(H_2O)_n$ and $CO_4^-(H_2O)_n$ increased continuously. This fact highlights two considerations. First, the binary reactions a-2-1, a-2-2, and b-2-1 of $CO_x^-(H_2O)_n$ to form $NO_x^-(H_2O)_n$ seem to occur infrequently. Therefore, the charge transfer reactions a-1-2 and b-1-2 might be the main reactions which form $NO_x^-(H_2O)_n$ in air. Second, the association reactions a-2 and b-2 of the primary ions with $CO_2$ are likely to proceed more frequently than reactions a-1 and b-1 with $H_2O$, when there is sufficient abundance of the primary ions in air. Thus the reactions a-1 and b-1 may become the source of $NO_x^-(H_2O)_n$ ion formation. The reason for the dominance of reaction a-2 over a-1 is that the bond strength between $O^-$ and $CO_2$ is stronger than that between $O^-$ and $H_2O$ [3]. Therefore the product ion of reaction a-2, $CO_3^-(H_2O)_n$, would exist more stably in air than the product ion of reaction a-1, $OH^-(H_2O)_n$. It has been pointed out, in fact, that trace amounts of $CO_2$ in air is important for negative ion formation. Shahin [8], Gardiner et al. [9], Skalny et al. [10], and Skalny [11] observed the dominance of the $CO_3^-$ ion at pressures from 6.7 up to 101 kPa, from 1.3 up to 4 kPa, from 5 up to 20 kPa, and from 5 up to 20 kPa, respectively.

Finally, the formation of a neutral by-product $HNO_3$ was confirmed at voltages above −3.0 kV (Fig. 5). The ion $HNO_3^-$ forms *via* reaction d-1 where $NO_2$ reacts with an OH radical followed by an electron attachment reaction (d-2 in Fig. 6) [12]. The radical species OH is most likely to be produced as one of the by-products of discharge and *via* the charge transfer reaction a-1-2 of $OH^-$ to $NO_2$. It has been described [12] that negative ions in air efficiently converted to $NO_3^-$ through any reaction with $HNO_3$, as shown in the reaction d-3 in Fig. 6. This is suggested from the fact that the abundances of $HNO_3^-$ and $NO_3^-(H_2O)_n$ increased simultaneously at a voltage of −3.0 kV.

## 4. Conclusions

Here we have reported the influence of needle voltage in the corona discharge on the formation of negative core ions $Y^-$ and their hydrated clusters $Y^-(H_2O)_n$ using APCDI MS with an insect pin as the corona needle. The use of APCDI MS in ambient air led to the finding of the "first hydrated shell" $OH^-(H_2O)_3$ (*m*/*z* 71) corresponding to $H_3O^+(H_2O)_3$ (*m*/*z* 73) which is a particularly stable form postulated by Eigen [18]. Various different core ions or their hydrates appeared according to the voltage applied on the needle for negative corona discharge. The use of the lowest and highest voltages in corona discharge resulted in the formation predominantly of hydrated cluster ions $OH^-(H_2O)_n$ and $NO_3^-(H_2O)_n$, respectively. The fact that $O_2^-(H_2O)_n$ was not observed, but $OH^-(H_2O)_n$ appeared at the lowest voltage suggested that the experimental conditions here were suitable for detecting the core ions formed in a reaction time longer than $10^{-3}$ s. It is interesting that $NO_3^-$ which is the longest-lived negative core ion [12] appeared at the highest needle voltage. This may suggest that the needle voltage or the electric field strength on the needle tip is related to the ion ageing time, although this could not be readily proved. Further study of the influence of electric field strength on the ion–molecule reactions relating to the production of primary ions, core ions, hydrated ions, and ion evolution, experimentally and theoretically is necessary. Especially, it is necessary to have more optimized conditions with respect to the discharge gap, the needle angle on the orifice plate, and the orifice size in i.d. and length. Such a study will help in the understanding the role of needle voltage in the formation of various different negative core ions and their hydrated clusters.

## References

[1] F. Yu, R.P. Turco, Geophys. Res. Lett. 27 (2000) 883.
[2] F. Yu, R.P. Turco, J. Geophys. Res. 106 (2001) 4797.
[3] F.C. Fehsenfeld, E.E. Ferguson, J. Chem. Phys. 61 (1974) 3181.
[4] H. Heitmann, F. Arnold, Nature 306 (1983) 747.
[5] M.D. Perkins, F.L. Eisele, J. Geophys. Res. 89 (1984) 9649.
[6] H. Kawamoto, T. Ogawa, Planet. Space Sci. 34 (1986) 1229.
[7] A. Luts, J. Geophys. Res. 100 (1995) 1487.
[8] M.M. Shahin, Appl. Opt. Suppl. Electrophotogr. 3 (1969) 106.
[9] P.S. Gardiner, J.D. Craggs, J. Phys. D: Appl. Phys. 10 (1977) 1003.
[10] J.D. Skalny, T. Mikoviny, S. Matejcik, N.J. Mason, Int. J. Mass Spectrom. 233 (2004) 317.
[11] J.D. Skalny, Acta Phys. Univ. Comen. 28 (1987) 161.
[12] K. Nagato, Y. Matsui, T. Miyata, T. Yamauchi, Int. J. Mass Spectrom. 248 (2006) 142.
[13] B. Gravendeel, F.J. de Hoog, J. Phys. B: At. Mol. Phys. 20 (1987) 6337.
[14] C.A.M. de Vries, F.J. Hoog, D.C. Sharam, Proceedings of the Sixth ISPC, Montreal, 1983, p. 317.
[15] S.K. Ross, A.J. Bell, Int. J. Mass Spectrom. 218 (2002) L1.
[16] L.B. Loeb, A.F. Kip, G.G. Hudson, Phys. Rev. 60 (1941) 714.
[17] S. Wei, Z. Shi, A.W. Castleman Jr., J. Chem. Phys. 94 (1991) 3268.
[18] M. Eigen, Angew Chem. Int. Ed. 3 (1964) 1.
[19] Y.K. Lau, S. Ikuta, P. Kebarle, J. Am. Chem. Soc. 104 (1982) 1462.
[20] M. Meot-Ner, C.V. Speller, J. Phys. Chem. 90 (1986) 6616.
[21] W.H. Robertson, E.G. Diken, E.A. Price, J.-W. Shin, M.A. Johnson, Science 299 (2003) 1367.
[22] F.C. Pickard IV., E.K. Pokon, M.D. Liptak, G.C. Shields, J. Chem. Phys. 122 (2005) 024302.
[23] F.C. Fehsenfeld, C.J. Howard, A.L. Schmeltekopf, J. Chem. Phys. 63 (1975) 2835.
[24] F.C. Fehsenfeld, E.E. Ferguson, D.K. Bohme, Planet. Space Sci. 17 (1969) 1759.
[25] N.G. Adams, D.K. Bohme, D.B. Dunkin, F.C. Fehsenfeld, E.E. Ferguson, J. Chem. Phys. 52 (1970) 3133.